Computers, Materials & Continua

Tech Science Press

Doi:10.32604/cmc.2025.067639

ARTICLE

Short-Term Multi-Hazard Prediction Using a Multi-Source Data Fusion Approach

Syeda Zoupash Zahra[1], Najia Saher[2], Malik Muhammad Saad Missen[3], Rab Nawaz Bashir[4,5], Salma Idris[5], Tahani Jaser Alahmadi[6,*] and Muhammad Inshal Khan[5]

[1]Deptment of Information Technology, The Islamia University of Bahawalpur, Bahawalpur, 63100, Pakistan
[2]Deptment of Artificial Intelligence, The Islamia University of Bahawalpur, Bahawalpur, 63100, Pakistan
[3]Deptment of Software Engineering, The Islamia University of Bahawalpur, Bahawalpur, 63100, Pakistan
[4]Department of Computer Science, COMSATS University Islamabad, Vehari Campus, Vehari, 61100, Pakistan
[5]Artificial Intelligence and Data Analytics Laboratory (AIDA), College of Computer and Information Sciences (CCIS), Prince Sultan University, Riyadh, 12435, Saudi Arabia
[6]Department of Information Systems, College of Computer and Information Sciences, Princess Nourah bint Abdulrahman University, Riyadh, 11671, Saudi Arabia

*Corresponding Author: Tahani Jaser Alahmadi. Email: tjalahmadi@pnu.edu.sa

Received: 08 May 2025; Accepted: 22 July 2025; Published: 23 October 2025

ABSTRACT: The increasing frequency and intensity of natural disasters necessitate advanced prediction techniques to mitigate potential damage. This study presents a comprehensive multi-hazard early warning framework by integrating the multi-source data fusion technique. A multi-source data extraction method was introduced by extracting pressure level and average precipitation data based on the hazard event from the Cooperative Open Online Landslide Repository (COOLR) dataset across multiple temporal intervals (12 h to 1 h prior to events). Feature engineering was performed using Choquet fuzzy integral-based importance scoring, which enables the model to account for interactions and uncertainty across multiple features. Three individual Long Short-Term Memory (LSTM) models were trained for hazard location, average precipitation, and hazard category (i.e., to detect the potential of natural disasters). These models were trained on varying temporal scales from 12 to 1 h prior to the event. These individual models achieved the performance of Mean Absolute Error (MAE) 2.2 and 3.2, respectively, for the hazard location and average precipitation models, and an F1-score of 0.825 for the hazard category model. The results also indicate that the LSTM model outperformed traditional Machine Learning (ML) models, and the use of the fuzzy integral enhanced the prediction capability by 8.12%, 2.6%, and 6.37%, respectively, for all three individual models. Furthermore, a rule-based algorithm was developed to synthesize the outputs from the individual models into a 3 × 3 grid of multi-hazard warnings. These findings underscore the effectiveness of the proposed framework in advancing multi-hazard forecasting and situational awareness, offering valuable support for timely and data-driven emergency response planning.

KEYWORDS: Time series prediction; machine learning; spatio-temporal data; multi-hazard prediction

1 Introduction

The frequency and severity of natural disasters, such as landslides and extreme precipitation, are increasing, raising significant concerns for infrastructure and communities worldwide [1]. Due to the inherent complexity and uncertainty of the risks generated by these events, it is imperative to provide timely and precise hazard warnings to mitigate them. The uncertainties and intricacies of multi-hazard scenarios present challenges to current systems [2]. This research contributes to addressing a significant gap in the field by establishing a framework that can incorporate a variety of environmental data to improve the precision of multi-hazard warnings. This study is of great importance in protecting vulnerable populations, enhancing disaster preparation and response, and mitigating potential losses.

The multi-hazard data-driven approaches are categorized into stochastic [3], empirical [4], and mechanistic models [5], each with its own strengths and limitations [6]. Stochastic models, such as multivariate models or copula-based techniques [7], effectively capture the complex relationships and dependencies between hazards [8]. However, they are not as effective in scenarios with sparse or uncertain data. The efficacy of extreme value and vine copulas in tail dependence analysis often makes it difficult to comprehend dynamic interactions among multiple hazards. Empirical models [9], including regression techniques and dependence measures, are implemented during the development of models to optimize computational efficiency and investigate hazard relationships. Regression models associated with the use of Linear and Logistic Regression [10] models are frequently used for the analysis of hazard dependencies while risking oversimplifying complex interactions. Measures such as tail dependence [11] and rank correlation [12] are used to determine the feats of dependencies but have no provision for learning from experience. Techniques such as Decision Tree [13], Support Vector Machine (SVM) [14], provide a higher level of flexibility compared to other techniques but rely heavily on large datasets and lack capability in terms of interpretable models in the geospatial-temporal context. Hazards are frequently oversimplified in interactions, relying heavily on prior experience and failing to accurately represent nonlinear or spatiotemporal complexities [15]. Mechanistic models, such as hydrological or climate-based physical models, can generate detailed hazard simulations [16]. However, they are computationally expensive and are susceptible to the uncertainties of the parameters involved, particularly in environments that are swiftly changing. Therefore, these obstacles necessitate hybrid models that integrate the advantages of these categories. As the model involves multiple heterogeneous data sources, accurately calculating feature importance becomes critical for effective prediction. Fuzzy integral techniques were selected because they account for interactions among features and manage uncertainty more robustly than traditional methods. This allows for adaptive weighting, enhancing the model's reliability in complex multi-hazard environments.

In this study, we propose a novel multi-source data fusion approach for forecasting multi-hazard warnings that attempts to overcome the limitations of existing traditional methods. The idea for the proposed model is to improve the accuracy and reliability of short-term predictions for landslides and extreme precipitation. The key contributions of the proposed model are outlined below:

- A novel data integration framework for short-term landslide and extreme precipitation warnings is presented, integrating precipitation data, Cooperative Open Online Landslide Repository (COOLR) data, and atmospheric pressure level data.
- The model uses fuzzy integral techniques for feature importance determination and the usage of weights that enable efficient allocation of weights given the uncertainty in environmental data.
- To enhance multi-hazard prediction, we apply a novel deep learning-based approach to predict potential geographic coordinates (latitude and longitude) with which landslides are associated, and estimate average precipitation rates.

This integrated approach fills key gaps in traditional forecasting systems to provide more accurate, and actionable, early warnings.

The sections of the study are arranged as follows: Section 2 provides a comprehensive review of the existing literature. Section 3 presents the data extraction process along with feature importance and model development. Section 4 discusses the outcomes of the study. Section 5 presents the concluding insights and future research directions.

2 Related Work

Robust modeling techniques that can capture the complicated interactions between different natural events are required to precisely predict multi-hazard risks. Data-driven models have become very successful in domains where we see success in recent years [17,18]. Some advantages of their method include computational efficiency and adaptivity to environmental behavioral factors, allowing for more accurate and dynamic predictions.

2.1 Empirical Methods for Hazard Prediction

Empirical methods for hazard prediction rely on data-driven techniques, using historical observations to establish relationships between variables. In the study [19], a discrete element model is used to investigate the failure and structural behaviour in the stepped reinforced soil retaining wall subject to loading conditions in which the patterns of force chains are used to determine any possible failure surfaces. The study [20], experiment is based on the combination of microseismic monitoring with numerical simulation to forecast the risk of rockburst in coal mining, which allows determining the precursors of the rockburst risk like the temporal changes of the energy index and the stress concentration zones to predict the early hazard.

Recent research also shows how satellite imagery is applied in the identification of landslides and in the assessment of risks. Ghorbanzadeh et al. [21] have applied ResU-Net and Object-Based Image Analysis (OBIA) integration to improve the quality of landslide maps with higher accuracy. Slope image stability analysis is done with the use of deep learning by Azmoon et al. [22] and proved to be effective for large-scale hazards. In their study, Mohan et al. [23] assessed the use of Convolutional Neural Networks (CNNs) and remote sensing images for identifying landslides with high spatial resolution and pointed out that even though the approach works well in recognizing spatial features, issues such as limited sample sizes exist. These studies demonstrate that satellite imagery is an effective tool for compiling geospatial data for the purpose of making accurate and large-scale hazard assessments.

2.2 Multi Hazard Prediction Models

Multi-hazard prediction, a complex process with implications in disaster management, is an important research field that requires more attention. Other challenges include the incorporation of multiple factors, such as climatic, geological, and hydrological factors, data limitations, and space-time dimensions. Such problems significantly hinder the development of reliable predictive models. Nevertheless, sophisticated techniques such as data-based techniques, machine learning (ML) techniques, and combined methods have greatly contributed to the development of multi-hazard forecasting.

Ali et al. [24] assessed fuzzy multi-criteria and ML methods and established that the Random Forest was more effective than other methods in landslide susceptibility assessment. Pourghasemi et al. [25] employed Random Forest model to produce multi-hazard probability maps of floods, landslides, and forest fires with high accuracy, but they mentioned the data-dependent issue. The study [26] also presented the coupled use of Geographic Information Systems (GIS) and ML for landslide, flood, and forest fire alerting and the importance of consistent data and methods. The works discussed here present a methodological pluralism of approaches and raise issues that pertain to the quality of data as well as the cross-hazard compatibility of data.

Despite numerous advances in multi-hazard prediction, substantial gaps persist in integrating multiple datasets and uncertainty in environmental factors. Most current methods lack frameworks that can correctly put heterogeneous data together, like precipitation, landslide records, and atmospheric conditions, for short-term hazards. In addition, existing approaches often have difficulties precisely defining spatial associations of hazards and dealing with uncertainties inherent in environmental data. To address these gaps, this study presents a novel data integration framework utilizing fuzzy integrals for feature importance and weight allocation. Furthermore, a ML-based technique improves the geographic precision of landslide prediction along with precipitation rate calculation.

3 Proposed Methodology

The methodology of this study comprises four key steps designed to develop a robust multi-hazard early warning framework. These steps are outlined below:

- **Data Extraction:** Relevant features such as pressure levels, average precipitation, elevation, and hazard attributes were extracted from the Climate Data Store (CDS) based on COOLR dataset across multiple time intervals prior to hazard events.
- **Data Fusion and Feature Importance Using Fuzzy Integral:** The Choquet fuzzy integral was applied to assess and aggregate the importance of heterogeneous features, enabling effective fusion of multi-source inputs.
- **Predictive Modeling:** Three distinct ong Short-Term Memory (LSTM) models were trained to forecast hazard location, average precipitation, and hazard category based on temporally fused features.
- **Integration into Multi-Hazard Warning Grid:** Outputs from the three LSTM models were synthesized using a rule-based approach to generate a 3 × 3 multi-hazard risk grid, indicating potential severity and overlap of multiple hazards.

3.1 Problem Statement

This study mapped the multi-hazard warning to a time series problem as forecasting $P(MHW_{T+1})$ by distributing it into regression and classification subtasks.

Let D represent the dataset, where each entry $d_i \in D$ consists of historical data from times $t_0, t_1, t_2, \ldots, t_n$. Each entry is associated with features that describe environmental, atmospheric, and geospatial conditions at these times. The probability of a multi-hazard warning at time $T+1$, denoted as $P(MHW_{T+1})$, is a function of the historical data:

$$P(MHW_{T+1}) = f(d_t, d_{t-1}, \ldots, d_{t-n}) \tag{1}$$

where f is a predictive model developed using ML techniques. For regression, the model predicts specific continuous variables such as the location of a potential landslide and the average precipitation rate:

3.2 Data Extraction

This study utilizes multi-source data that includes environmental, atmospheric, and geospatial data. The NASA Global Precipitation Measurement (GPM) is the data provider for the COOLR [27]. COOLR serves as a useful tool for analyzing landslide events and their relationships with precipitation information. The COOLR dataset is used as the primary source of data along with other datasets including satellite precipitation data [28] and pressure level data [29]. The COOLR dataset comprises 11,033 records from 140 distinct countries. This study concentrated on 'US' events, which comprise 2992 records. The COOLR dataset is used to extract the event date and time, as well as its location (longitude and latitude). Based on the date, time, and location provided, satellite precipitation data and pressure level data are extracted from the CDS [30] up to 24 h early from the event interval. A dynamic grid policy is adopted to create a 3 × 3 grid centered on the event location based on the COOLR dataset. This dynamic grid is further used for the satellite precipitation and pressure level data extraction.

Satellite precipitation data, available on a daily mean basis, is extracted for analysis using both 12-h and 24-h mean intervals. This extraction then allows for a more granular view of precipitation patterns, including shorter-term variations (12 h mean) as well as daily scale trends (24 h mean).

Reanalysis pressure level data is available at 1-h time intervals for 16 different variables and 37 different isobaric planes. The pressure level data extraction process in this study involves the extraction of 11 distinct variables for a single isobaric plane (1000 hPa) at five distinct time intervals, ranging from 1-h to 12-h prior to the event, as illustrated in Fig. 1.

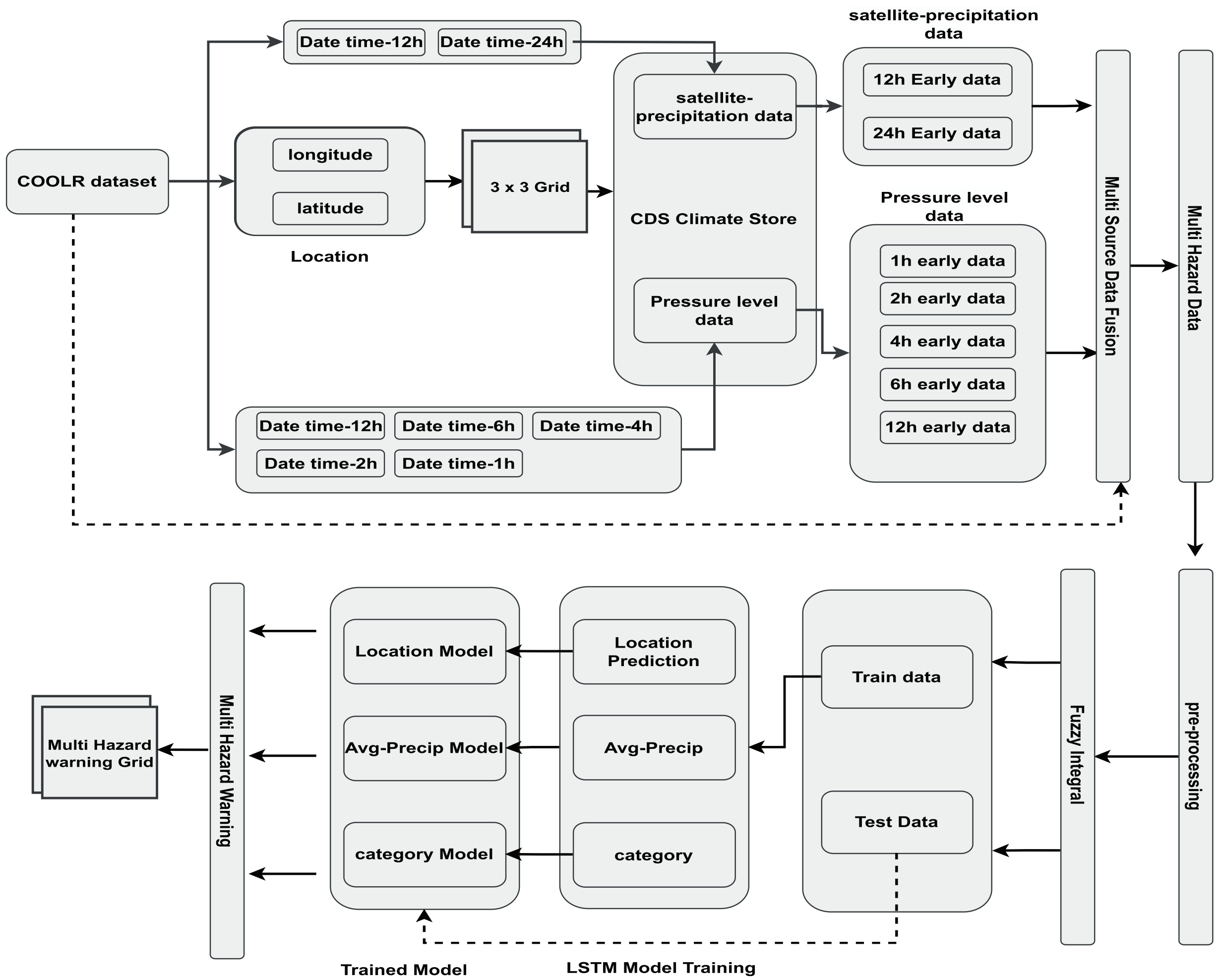

Figure 1: Overview of data extraction and predictive modeling workflow for multi-hazard warning

3.3 Data Fusion and Feature Importance Using Fuzzy Integral

The use of multiple datasets is especially important for an efficient analysis of multi-hazard risk assessment. In this research, we use a data fusion approach based on a unique ID that is attached to each event:

- D_{land} represents the COOLR dataset containing landslide event data.
- $D_{pressure}$ represents the dataset with atmospheric pressure levels recorded at multiple time intervals before an event.
- D_{precip} represents the dataset detailing average precipitation data before an event.

Each dataset D_i contains records $R_{i,j}$ indexed by j, with each record comprising a unique identifier $id_{i,j}$ and a set of features $F_{i,j}$. The fusion function F integrates records from these datasets based on the common identifier id. This function is defined as:

$$F(R_{\text{land},k}, R_{\text{pressure},k}, R_{\text{precip},k}) = \{id_k\} \cup F_{\text{land},k} \cup F_{\text{pressure},k} \cup F_{\text{precip},k} \quad (2)$$

where $R_{land,k}$, $R_{pressure,k}$, $R_{Precip,k}$ are records from the landslide, pressure, and precipitation datasets, respectively, corresponding to the same event k. The fuzzy integral is used in order to apply and calculate the importance of features with the help of the Choquet integral. This approach allows for a more realistic evaluation of the significance of the features, following the interactions between the features within a dataset. The foundation of feature importance measurement, g_i, which is stated in Eq. (3), comes from a Random Forest model. This score provides insights as to how predictively useful and impactful each feature from the dataset is and establishes a baseline for subsequent fuzzy integral method computations.

$$g_i = \text{importance of feature } i \text{ from Random Forest} \quad (3)$$

$$\mu_i = \frac{g_i}{\sum_{j=1}^{n} g_j} \quad (4)$$

where μ_i represents the normalized importance measure for the i-th feature. It is calculated by dividing the raw importance g_i by the sum of all feature importances, ensuring that the sum of all μ_i equals 1. This normalization allows for the fair comparison and aggregation of feature importances.

$$C_\mu(X) = \sum_{i=1}^{n} (x_{(i)} - x_{(i-1)}) \cdot \mu(A_{(i)}) \quad (5)$$

The Choquet integral $C_\mu(X)$ is computed using the sorted features and their cumulative measures. Here, $x_{(i)}$ is the i-th largest feature value, $x_{(i)}$ is the feature value preceding $x_{(i)}$, and $\mu(A_{(i)})$ denotes the fuzzy measure (importance) of the subset of features whose values are at least $x_{(i)}$. Physically, $\mu(A_{(i)})$ represents the collective importance or weight of all features that contribute at or above a given threshold in the prediction process. This integral aggregates the weighted contributions of all features. Feature values are sorted in descending order according to their normalized importance μ. However, it is necessary to sort the features since the application of the Choquet integral is based on using ordered feature values.

$$\text{sorted}_X = \text{sort}(X, \text{descending by } \mu) \quad (6)$$

sorted_measures assigns the corresponding normalized measures μ to the sorted features such that each feature is also aligned with the feature importance.

$$\text{sorted\_measures} = \mu \text{ (corresponding to sorted}_X) \quad (7)$$

Calculates the cumulative maximum of the sorted feature array. It is essential for the Choquet integral computation, which uses the maximum value at each step to scale the differences in feature values.

$$\text{cum\_max} = \text{cumulative\_max}(\text{sorted}_X) \quad (8)$$

ci_values calculates the Choquet integral, which combines the contributions of each feature. It sums the products of the differences in sorted measures and the cumulative maxima, effectively aggregating the feature importances in a non-linear manner based on their sorted importance.

$$\text{ci\_values} = \sum_{i=1}^{n} (\text{sorted\_measures}_i - \text{sorted\_measures}_{i-1}) \cdot \text{cum\_max}_i \quad (9)$$

3.4 Predictive Model

In the Predictive Modeling section of this study, we delve into the development and application of three distinct LSTM models, each tailored to predict specific aspects of multi-hazard scenarios: average precipitation, hazard category, and hazard location. The data is carefully split into training and testing sets so that we have a robust methodology for training and validating the model. As such, these models form the basis of a more complete multi-hazard warning system that issues exact, spatially explicit, actionable warnings through a 3 × 3 grid approach. Each model consists of 2 LSTM layers with 64 hidden units and a dropout rate of 0.5. The models are trained using the Adam optimizer with a learning rate of 0.001, a batch size of 64, and 200 epochs.

3.4.1 Integration into Multi-Hazard Warning Grid

Predictions from three specialized LSTM models (location $\hat{Y}_{\text{loc}}$, category $\hat{Y}_{\text{precip}}$, precipitation $\hat{Y}_{\text{cat}}$) are composited in the multi-hazard warning system and used to produce synthesized hazard warnings. The precipitation model $\hat{Y}_{\text{precip}}$ calculates the risk of flash floods, whereas the location model $\hat{Y}_{\text{loc}}$ points out where potential hazard sites are, and the category model determines what type of hazard (e.g., landslide or mudslide) $\hat{Y}_{\text{cat}}$ is involved. They forecast on a 3 × 3 grid about the predicted hazard location with a warning area inside of there. These data points are integrated using a rule-based approach with predefined criteria to determine the severity and type of hazard, including a single or compound hazard, to arrive at the multi-hazard warning.

The predictions of $\hat{Y}_{\text{loc}}$, $\hat{Y}_{\text{precip}}$ and $\hat{Y}_{\text{cat}}$ are used for the prediction of the multi-hazard warning grid as shown in Algorithm 1.

Algorithm 1: Rule-based multi-hazard warning

Require: $\hat{Y}_{\text{loc}}$, $\hat{Y}_{\text{precip}}$, $\hat{Y}_{\text{cat}}$
Ensure: Multi-hazard risk level (Low, Medium, High)
procedure **CATEGORIZEPRECIP** (*precip*)
    $quantiles \leftarrow$ calculate quantiles at $[0.33, 0.66]$
    if $precip \le quantiles[0.33]$ **then**
        return Low
    else if $precip \le quantiles[0.66]$ **then**
        return Medium
    else
        return High
    end if
end procedure
procedure ASSESSRISK (*precipCategory, hazardType*)
    if $(precipCategory = \text{Low}) \wedge (hazardType = \text{Landslide})$ **then**
        return Low
    else if $(precipCategory = \text{Low}) \wedge (hazardType = \text{Mudslide})$ **then**
        return Medium

(Continued)

Algorithm 1 (continued)

    else if $(precipCategory = \text{Medium}) \wedge (hazardType = \text{Landslide})$ **then**
        return Medium
    else if $(precipCategory = \text{Medium}) \wedge (hazardType = \text{Mudslide})$ **then**
        return High
    else if $(precipCategory = \text{High})$ **then**
        return High
    end if
end procedure
$precipData \leftarrow$ Load precipitation data
for each event in dataset **do**
    $precipCategory \leftarrow$ CategorizePrecip$(event.precip)$
    Compare $\hat{Y}_{\text{precip}}$ with *precipCategory*
    $predictedCategory \leftarrow$ Find category for $\hat{Y}_{\text{precip}}$
    Use *predictedCategory* for the next step
    $hazardType \leftarrow \hat{Y}_{\text{cat}}$
    $risk \leftarrow$ AssessRisk$(predictedCategory, hazardType)$
    Record the risk level for the event
end for
Generate 3 × 3 Grid around $\hat{Y}_{\text{loc}}$:
Define central point as $\hat{Y}_{\text{loc}}$
Generate surrounding points in a 3 × 3 grid:
  grid $\leftarrow \{(x, y) \mid x, y \in \{-1, 0, 1\}, (x, y) \neq (0, 0)\}$
for each grid point (x_i, y_i) **do**
    Calculate corresponding risk level based on *precipCategory* and *hazardType*
    Assign risk level to the grid cell
end for
Output the grid with associated risk levels

4 Evaluation

It is important to assess the performance of the predictive models as well as the multi-hazard warning system to determine their efficiency and credibility in practice. This section describes the methods and measures to calculate the accuracy, precision, and operational performance of the developed models under different environments and hazardous events.

4.1 Results

In order to evaluate the effectiveness of the proposed methodology, we answer the questions presented earlier in this section. Individual models are studied in detail, and the integrated multi-hazard warning system is assessed in terms of performance.

4.1.1 Performance of Individual Predictive Model

To evaluate the performance of each individual model $\hat{Y}_{\text{loc}}$, $\hat{Y}_{\text{precip}}$, $\hat{Y}_{\text{cat}}$ corresponding evaluation metrics are utilized on the test data as shown in the Table 1.

Table 1: Hazard location, precipitation, and category prediction models from (12 h to 1 h) early data fusion

Hazard location				Avg precipitation		Hazard category		
Model	**Event-time**	**MAE**	R^2	**MAE**	R^2	**Precision**	**Recall**	**F1-score**
LSTM	12 h	4.1	0.65	6.66	0.58	0.688	0.693	0.68
LSTM	12 h + 6 h	3.7	0.70	6.1	0.60	0.69	0.71	0.699
LSTM	12 h + 6 h + 4 h	3.1	0.75	5.5	0.64	0.74	0.73	0.734
LSTM	12 h + 6 h + 4 h + 2 h	2.7	0.82	4.0	0.70	0.76	0.77	0.764
LSTM	12 h + 6 h + 4 h + 2 h + 1 h	2.2	0.89	3.2	0.76	0.82	0.83	0.825

Table 1 column (Hazard location) shows the results of the performance of the LSTM model in estimating hazard locations at different intervals of time prior to the event. The "Event-time" labels such as "12 h + 6 h" represent the fusion of data collected at multiple distinct temporal intervals prior to the event. Increasing the granularity of the time intervals leads to major improvements in both Mean Absolute Error (MAE) and the coefficient of determination (R^2). Specifically, if the model is trained with data from shorter time intervals (12 h down to 1 h) before the event, the MAE and R^2 are equal to 4.1 and 0.65, respectively, down to 2.2 and 0.89.

Table 1 column (Avg Precipitation) shows how the LSTM model predicts average precipitation and how the MAE drops remarkably from 6.66 to 3.2 when temporal layers from 12 h before the event to 1 h before the event are added, and how the R^2 value also increases from 0.58 to 0.76. This enhancement results in a more accurate prediction and model robustness with finer temporal resolution of the data inputs. The performance visualization can be seen in Fig. 2.

Figure 2: Comparative analysis for hazard location, average precipitation and hazard category prediction models over time

It can be observed from Table 1 column (Hazard Category) that there is a gradual increase in Precision, Recall, and F1-Score from a timestamp of 12 h before the event to the timestamp of 1 h prior to the event. The Precision and Recall of the model rose from around 0.69 to 0.83, and the F1-Score rose from 0.68 to 0.825, indicating a noticeable increase in both accuracy and the average of precision and recall values as event time distance is reduced as shown in Fig. 2.

4.1.2 Impact of the Fuzzy Integral

As shown in the results in Table 2, the application of fuzzy integral-based feature importance to the predictive model has a significant effect. Fuzzy integrals reduce the MAE of the Location model by 8.18% and improve R^2 from 0.82 to 0.89, a 24% increase in R^2. The Avg-Precip model also improved R^2 from 0.74 to 0.76, with a decrease in MAE by 11.76%.

Table 2: Perforamnce of individual models with and without Fuzzy integral

Prediction type	Fuzzy integral	Precision	Recall	F1-score	MAE	R^2
Location	No	–	–	–	2.8	0.82
	Yes	–	–	–	**2.2**	**0.89**
Avg-precip	No	–	–	–	3.6	0.74
	Yes	–	–	–	**3.2**	**0.76**
Category	No	0.79	0.76	0.774	–	–
	Yes	**0.82**	**0.83**	**0.825**	–	–

Improvements were observed across all classification metrics (Precision, Recall, and F1-Score) for the Category model, with an increase in the F1-Score from 0.774 to 0.825, representing a 6.37% improvement. These results demonstrate that fuzzy integral techniques are effective in improving model performance by prioritizing more important features, thereby enhancing the predictive capabilities of multi-hazard warning systems.

4.1.3 Performance of LSTM Model

Table 3 shows comparative performance analysis across different predictive models highlights LSTM's superior capability, particularly in terms of prediction accuracy for multi-hazard scenarios. LSTM is the best model for location prediction, achieving an MAE of 2.2 and R^2 of 0.89. Traditional ML models like Linear Regression and Decision Tree lag significantly behind, with lower R^2 values, showcasing LSTM's ability to successfully deal with temporal dependencies in location data. LSTM again takes the lead with the lowest MAE (3.2) and solid R^2 in the Avg-precipitation prediction, also demonstrating the ability to capture the intrinsic properties in the precipitation pattern better than other ML models. The sheer nature of this disparity demonstrates that LSTM is well-equipped for handling and predicting through time series data, which traditional models can't deal with. For predicting the Category model, LSTM has the highest precision, recall, and F1 score, validating its role as the strongest in predicting hazard type. The LSTM's F1-Score of 0.825 is notably higher compared to other models like the Decision Tree and Extreme Gradient Boosting (XGB), which show comparable scores but do not reach the LSTM's performance level as shown in Fig. 3. These results collectively establish that LSTM not only achieves superior predictive accuracy but is a valid modeling approach for multiple aspects of hazard prediction and therefore is uniquely suitable for the combined task of multi-hazard warning systems.

Table 3: Performance of LSTM model compared to other ML models

Prediction type	Model	Precision	Recall	F1-score	MAE	R^2
Location	LR	–	–	–	6.2	0.37
	Decision tree	–	–	–	3.6	0.65
	Random forest	–	–	–	2.6	0.76
	XGB	–	–	–	2.7	0.76
	LSTM	–	–	–	**2.2**	**0.89**
Avg-precip	LR	–	–	–	8.1	0.27
	Decision tree	–	–	–	4.6	0.59
	Random forest	–	–	–	3.6	0.74
	XGB	–	–	–	3.3	0.75
	LSTM	–	–	–	**3.2**	**0.76**
Category	LR	0.58	0.62	0.599	–	-
	Decision tree	0.76	0.77	0.765	–	-
	Random forest	0.76	0.78	0.77	–	-
	XGB	0.77	0.77	0.77	–	-
	LSTM	**0.82**	**0.83**	**0.825**	–	–

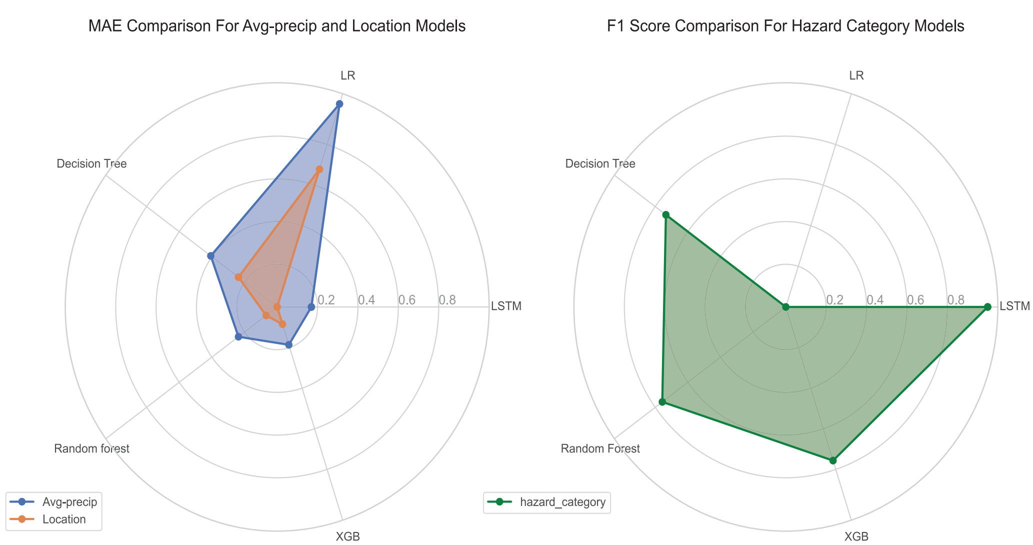

Figure 3: Radar charts comparing MAE and F1 score across ML models for location and average precipitation predictions

4.1.4 Multi-Hazard Warning

To evaluate the process of the multi-hazard warning using the individual models, a real-time example is used to describe the process. The performance of the individual models is analyzed based on the hazard id: 8133. This hazard occurred on OR 47, milepost 86.8, USA, at 12/7/2015 20:38, having actual latitude and longitude [45.5664, –123.10631], respectively. For this hazard event, first analyze the prediction of the $\hat{Y}_{\text{loc}}$, $\hat{Y}_{\text{precip}}$, $\hat{Y}_{\text{cat}}$ then based on the Algorithm 1 calculate the multi-hazard risk for the event. The predicted coordinates $\hat{Y}_{\text{loc}}$ for the possible hazard were [46.408356, –123.6038]. The predicted avg-precip $\hat{Y}_{\text{precip}}$ was 19.8246 and the predicted category $\hat{Y}_{\text{cat}}$ was a landslide. Based on the predicted values, the proposed model generates the 3×3 grid around the predicted location and generates the multi-hazard warning as high, as possible landslides can occur and extreme avg-precipitation can cause flash floods in the grid area. The process visualization can be seen in Fig. 4 which describe the effectiveness of the proposed model. That describes the effectiveness of the proposed model.

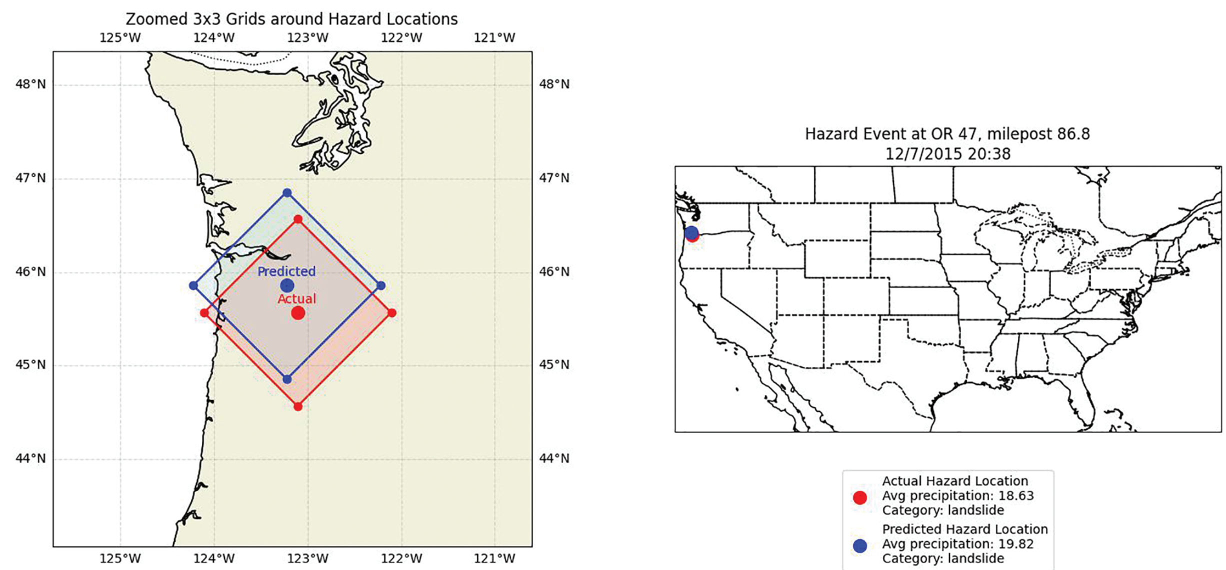

Figure 4: Comparison of actual and predicted event centers within a 3×3 hazard risk grid

The scientific strength of this work is the scientific rationality of the judicious combination of LSTM networks and the Choquet fuzzy integral in addressing the spatial and temporal complexity of multi-hazard prediction. The features of LSTM models make them especially well-suited to task of discovering time-variation across meteorological and hazard data that is not readily understood by traditional models. The fuzzy integral, in the meantime, allows to robustly fuse features covering both the importance of an individual feature and the interaction between them, which makes the representation of the data more subtle. Such synergy strengthens the overall generalization performance of the model in diverse lead times and hazard type rendering steady better performance and increased trustworthiness of early warning results.

5 Conclusion

This study proposed a novel multi-source data fusion framework incorporating fuzzy integrals and LSTM-based predictive models for short-term multi-hazard warnings, targeting landslide and extreme precipitation prediction. The proposed approach demonstrated strong predictive performance, achieving an MAE of 2.2 and an R^2 of 0.89 for hazard location prediction, an MAE of 3.2 and an R^2 of 0.76 for average precipitation forecasting, and an F1-score of 0.825 for hazard category classification, indicating high accuracy and robustness across all three predictive tasks. The outcomes also revealed that the LSTM model outperformed the traditional ML models, and incorporation of heterogeneous environmental, atmospheric and geospatial data through the fuzzy integral also improved the ability to predict by 8.1%, 2.6% and 6.37% on the location of the hazard, the forecasting of precipitation, and classification of hazard categories, respectively. In addition, a rule-based algorithm successfully incorporated the results of individual models into a localized assessment of multi-hazard risk level, presented in a spatial 3×3 risk grid, which was much more practical with regard to the scales of space and decision support. The study presents certain limitations, including dependence on the spatial resolution of the COOLR dataset, which may affect model performance in regions with limited data availability or differing climatic conditions. Moreover, real-time deployment poses challenges due to the computational demands of model complexity and extensive data preprocessing. Although this study mainly focuses on multi-source data fusion to improve the prediction of hazards, future work can be performed on how to integrate advanced deep learning architectures to enhance matching and flexibility. Moreover, the integration of real-time sensor information and maximizing model performance shall be critical toward facilitating scalable and functional early warning systems in diverse geographical environments.

Acknowledgement: The authors extend their appreciation to the Princess Nourah bint Abdulrahman University Researchers Supporting Project, Princess Nourah bint Abdulrahman University, Riyadh, Saudi Arabia. Authors are also thankful to Prince Sultan University, Riyadh Saudi Arabia for support of Article Processing Charges (APC) for this publication.

Funding Statement: The Princess Nourah bint Abdulrahman University Researchers Supporting Project number (PNURSP2025R513), Princess Nourah bint Abdulrahman University, Riyadh, Saudi Arabia.

Author Contributions: The research design, methodology development, data analysis and writing the manuscript were made by Syeda Zoupash Zahra, who was the first and the main author. Writing of the literature review and assisting in data interpretation was Najia Saher. Experimental validation and technical editing were done by Malik Muhammad Saad Missen. Data curation and formal analysis was made by Rab Nawaz Bashir and Salma Idris. The validation process of research was perform by Tahani Jaser Alahmadi and Muhammad Inshal Khan. All authors reviewed the results and approved the final version of the manuscript.

Availability of Data and Materials: The experimental code and extracted data for this study are available at the following GitHub repository: Multi-hazard project repository https://github.com/chkalim/multi_hazard (accessed on 21 July 2025).

Ethics Approval: Not applicable.

Conflicts of Interest: The authors declare no conflicts of interest to report regarding the present study.

References

1. Wang J, He Z, Weng W. A review of the research into the relations between hazards in multi-hazard risk analysis. Nat Hazards. 2020;104(3):2003–26. doi:10.1007/s11069-020-04259-3.
2. Roy T, Matsagar V. Multi-hazard analysis and design of structures: status and research trends. Struct Infrastruc Eng. 2023;19(6):845–74. doi:10.1080/15732479.2021.1987481.
3. Cox DR. The theory of stochastic processes. Abingdon, UK: Routledge; 2017.
4. Zou KH, Tuncali K, Silverman SG. Correlation and simple linear regression. Radiology. 2003;227(3):617–28. doi:10.1148/radiol.2273011499.

5. Devia GK, Ganasri BP, Dwarakish GS. A review on hydrological models. Aquatic Procedia. 2015;4(3):1001–7. doi:10.1016/j.aqpro.2015.02.126.
6. Tilloy A, Malamud BD, Winter H, Joly-Laugel A. A review of quantification methodologies for multi-hazard interrelationships. Earth-Sci Rev. 2019;196(3–4):102881. doi:10.1016/j.earscirev.2019.102881.
7. Latif S, Mustafa F. Copula-based multivariate flood probability construction: a review. Arab J Geosci. 2020;13(3):132. doi:10.1007/s12517-020-5077-6.
8. Owolabi TA, Sajjad M. A global outlook on multi-hazard risk analysis: a systematic and scientometric review. Int J Disaster Risk Reduct. 2023;92(278):103727. doi:10.1016/j.ijdrr.2023.103727.
9. Mir AA, çelebi FV, Rafique M, Hussain L, Almasoud AS, Alajmi M, et al. An improved imputation method for accurate prediction of imputed dataset based radon time series. IEEE Access. 2022;10(2):20590–601. doi:10.1109/access.2022.3151892.
10. Gorsevski PV, Gessler PE, Foltz RB, Elliot WJ. Spatial prediction of landslide hazard using logistic regression and ROC analysis. Trans GIS. 2006;10(3):395–415. doi:10.1111/j.1467-9671.2006.01004.x.
11. Lan M, Shao Y, Zhu J, Lo S, Ng ST. A hybrid copula-fragility approach for investigating the impact of hazard dependence on a process facility's failure. Process Safe Environm Protect. 2021;149(6183):1017–30. doi:10.1016/j.psep.2021.03.014.
12. Ghizzoni T, Roth G, Rudari R. Multivariate skew-t approach to the design of accumulation risk scenarios for the flooding hazard. Adv Water Resourc. 2010;33(10):1243–55. doi:10.1016/j.advwatres.2010.08.003.
13. Cramer GM, Ford RA, Hall RL. Estimation of toxic hazard—a decision tree approach. Food and Cosmetics Toxicology. 1976;16(3):255–76. doi:10.1016/s0015-6264(76)80522-6.
14. Hong H, Pradhan B, Xu C, Tien Bui D. Spatial prediction of landslide hazard at the Yihuang area (China) using two-class kernel logistic regression, alternating decision tree and support vector machines. CATENA. 2015;133:266–81. doi:10.1016/j.catena.2015.05.019.
15. Kappes MS, Keiler M, von Elverfeldt K, Glade T. Challenges of analyzing multi-hazard risk: a review. Nat Hazards. 2012;64(2):1925–58. doi:10.1007/s11069-012-0294-2.
16. Nashwan MS, Shahid S, Chung ES, Ahmed K, Song YH. Development of climate-based index for hydrologic hazard susceptibility. Sustainability. 2018;10(7):2182. doi:10.3390/su10072182.
17. Mujahid N, ARMFSAARK Muhammad Mujahid. Large language model in healthcare for the prediction of genetic variants from unstructured text medicine data using natural language processing. Comput Mater Continua. 2025;84(1):1883–99. doi:10.32604/cmc.2025.063560.
18. Ahmad Z, Mahmood T, Alam T, Rehman A, Saba T. Enhancing time series forecasting with an optimized binary gravitational search algorithm for echo state networks. IEEE Access. 2023;11:79466–79. doi:10.1109/access.2023.3292543.
19. Ma K, Wang L, Long L, Peng Y, He G. Discrete element analysis of structural characteristics of stepped reinforced soil retaining wall. Geomat Natural Hazards Risk. 2020;11(1):1447–65. doi:10.1080/19475705.2020.1797907.
20. Ma K, Wang H, Liao Z, Peng Y, Wang K. Precursor of microseismic energy and stress evolution induced by rockburst in coal mining: a case study from Xiashijie, Shannxi, China. Geomech Geophys Geo-Energy Geo-Resour. 2022;8(5):134. doi:10.1007/s40948-022-00435-w.
21. Ghorbanzadeh O, Shahabi H, Crivellari A, Homayouni S, Blaschke T, Ghamisi P. Landslide detection using deep learning and object-based image analysis. Landslides. 2022;19(4):929–39. doi:10.1007/s10346-021-01843-x.
22. Azmoon B, Biniyaz A, Liu Z, Sun Y. Image-data-driven slope stability analysis for preventing landslides using deep learning. IEEE Access. 2021;9:150623–36. doi:10.1109/access.2021.3123501.
23. Mohan A, Singh AK, Kumar B, Dwivedi R. Review on remote sensing methods for landslide detection using machine and deep learning. Trans Emerg Telecomm Technol. 2021;32(7):e3998. doi:10.1002/ett.3998.
24. Ali SA, Parvin F, Vojteková J, Costache R, Linh NTT, Pham QB, et al. GIS-based landslide susceptibility modeling: a comparison between fuzzy multi-criteria and machine learning algorithms. Geosci Front. 2021;12(2):857–76. doi:10.1016/j.gsf.2020.09.004.

25. Pourghasemi HR, Gayen A, Edalat M, Zarafshar M, Tiefenbacher JP. Is multi-hazard mapping effective in assessing natural hazards and integrated watershed management? Geosci Front. 2020;11(4):1203–17. doi:10.1016/j.gsf.2019.10.008.
26. Pourghasemi HR, Kariminejad N, Amiri M, Edalat M, Zarafshar M, Blaschke T, et al. Assessing and mapping multi-hazard risk susceptibility using a machine learning technique. Sci Rep. 2020;10(3203):1–11. doi:10.1038/s41598-020-60191-3.
27. Juang CS, Stanley TA, Kirschbaum DB. Using citizen science to expand the global map of landslides: introducing the Cooperative Open Online Landslide Repository (COOLR). PLoS One. 2019;14(7):e0218657. doi:10.1371/journal.pone.0218657.
28. Precipitation monthly and daily gridded data from 1979 to present derived from satellite measurements; 2021 [Internet]. [cited 2024 Dec 30]. Available from: https://cds.climate.copernicus.eu/datasets/satellite-precipitation?tab=overview.
29. Hersbach H, Bell B, Berrisford P, Hirahara S, Horányi A, Muñoz-Sabater J, et al. The ERA5 global reanalysis. Quart Je Royal Meteorolog Soc. 2020;146(730):1999–2049.
30. Raoult B, Bergeron C, Alós AL, Thépaut JN, Dee D. Climate service develops user-friendly data store. ECMWF Newslett. 2017;151:22–7.